Nuclear Data for Science and Technology (1988 MITO), 1185-1188, Copyright © 1988 JAERI.

DEVELOPMENT AND BENCHMARKING OF HIGHER ENERGY NEUTRON TRANSPORT DATA LIBRARIES

E. D. Arthur, P. G. Young, R. T. Perry, D. G. Madland, R. E. MacFarlane,
R. C. Little, M. Bozoian, and R. J. LaBauve

Theoretical and Applied Theoretical Physics Divisions
Los Alamos National Laboratory
Los Alamos, New Mexico, USA

Abstract: Neutron cross-section evaluations covering the energy range from 10^{-11} to 100 MeV have been prepared for several materials. The principal method used to generate this data base has employed statistical-preequilibrium nuclear models, sophisticated phase shift analyses, and R-matrix techniques. The library takes advantage of formats developed for Version 6 of the Evaluated Nuclear Data File, ENDF. Methods to efficiently utilize the ENDF/B-VI representation of this library in the MCNP Monte Carlo code have been developed. MCNP results using the new library have been compared with calculated results using codes or data based upon intranuclear cascade models.

(Keywords: Data evaluation, Higher energy, Statistical-preequilibrium model, ENDF/B-VI, MCNP, Benchmark calculations)

Introduction

This paper describes an extensive effort under way within the Applied Nuclear Science and Radiation Transport groups at Los Alamos National Laboratory to develop and implement neutron transport libraries covering the energy range from 10^{-11} to 100 MeV. This effort is aimed at producing both continuous energy and multigroup data libraries so that applications in both Monte Carlo and discrete-ordinates transport codes will be possible. The principal method used to generate this data base has employed statistical-preequilibrium nuclear models, sophisticated phase shift analyses, and R-matrix techniques. This is in contrast to previous efforts that were based upon intranuclear-cascade-evaporation (ICE) models, developed generally for very high energies (≥ 1 GeV), which were applied at much lower energies. Use of such ICE models at lower energies leads to conditions where their physical assumptions and calculated results may be suspect. In contrast, the theoretical methods listed above have been developed and tested for nucleon-nucleus reactions in the range of several tens of MeV. This paper will illustrate the validity of such models and the information produced from calculations using them through comparisons with neutron and proton-induced experimental data available for energies below 100 MeV. This library utilizes formats developed for the new version (Version 6) of the evaluated nuclear data file, ENDF, and specific examples of the utilization of new features of these formats will be presented, particularly in the context of new sampling algorithms for Monte Carlo calculations. Finally, results from transport benchmark calculations will be presented and compared with calculations obtained using ICE techniques.

Nuclear Models and Their Validation

The principal theoretical methods employed to produce the data libraries described here are based upon the preequilibrium-statistical model, although, as described in the Introduction, phase shift and R-matrix analyses were used in the case of neutron reactions with hydrogen. The mechanism for utilization of such a model is through implementation into the GNASH[1] nuclear model code system, along with other developments such as the generation of new optical parameter sets for nucleon-nucleus reactions in the energy range from 50-500 MeV. Most of the GNASH development is described in a companion paper[2] to this conference, while the optical model development is described in Ref. 3. Figure 1 illustrates the GNASH system used for the present effort. It allows a choice of Hauser-Feshbach, s-wave approximation,[4] or evaporation models, and uses identical input files (optical model transmission coefficients, nuclear-levels, direct-reaction cross-section data, and nuclear masses) and produces output files that are then transformed into ENDF-formatted files. For all models, one-step preequilibrium corrections are applied, while for evaporation and s-wave approximation models, multistage preequilibrium contributions are calculated. In addition to the angle-integrated spectra, activation yields, and gamma-ray lines calculated in the main GNASH module, the auxiliary modules ANGDIS, THKCODE, and GNFILE6 allow production of double differential spectra, thick target yields and spectra for incident charged particles, and ENDF/B file 6 formatted data,[5] respectively.

In order to assess the validity of the models discussed above, an extensive set of comparisons have been made with experimental data. Because of the paucity of neutron data above 20 MeV, many of these comparisons involve proton-induced thin- and thick-target data. Selected examples will be highlighted in the discussions that follow. An important source of data pertaining to particle emission spectra are found in 90-MeV (p,xp) and (p,xn) measurements made by Kalend et al.[6] Figure 2 compares GNASH calculations with angle-integrated proton and neutron spectra measured for p + ^{58}Ni reactions. The agreement is quite good, especially for emitted neutrons. Comparisons made to double-differential data measured in the same series of experiments also show good agreement, thereby confirming the validity of the angular-distribution systematics phenomenology developed by Kalbach[7] that were used extensively in the present effort. An additional source of proton-induced spectral data comes from thick target measurements such as those recently made by Kiziah et al.[8] Figure 3 compares 30-degree neutron spectra produced by 52-MeV protons stopping in a thick aluminum target with these new data. Again, the agreement is good and is significantly better than results obtained using intranuclear-cascade evaporation model techniques.

As described in Ref. 2, a significant amount of GNASH development has centered around techniques that will allow realistic calculations of gamma-ray production produced by high energy neutrons. Recently, new facilities, such as the Los Alamos WNR high energy neutron target (see contribution for this conference[9]) allow reliable gamma-ray production measurements to be made for neutron energies up to several hundred MeV. Data[10] are now just becoming available from this facility that are invaluable in benchmarking our calculational methods and techniques. Figure 4 compares, for n + ^{181}Ta reactions between 20 and 80 MeV, our calculated gamma-ray production cross section for gamma rays having energies greater than 2 MeV with the data of Ref. 10. Our calculations are in good agreement with these data. Also indicated in the figure by the dashed line is the total calculated production cross section for gamma rays having all energies. Because gamma-ray production measurements sample contributions from all reaction paths occurring at a particular incident energy, the comparisons shown here provide a stringent test of the models used in this energy regime.

Neutron Data Library Production

Using the theoretical methods briefly described here and presented in more detail in Ref. 2, ENDF-formatted data libraries describing neutron reactions have been produced that cover the energy range from 10^{-11} to either 50 or 100 MeV. Materials for which such libraries now exist are listed in Table 1. These libraries include neutron total, elastic, and nonelastic cross sections, angular distributions for elastic scattering, as well as production cross sections for neutrons, protons, deuterons, alphas, and gamma rays, with their associated energy-angle spectra. Specific representation of correlated energy-angle cross sections utilizes the new File 6 representation of ENDF, and is an essential feature necessary to describe strong forward peaking occurring at higher energies. Although the main emphases here are energies between 20 and 100 MeV, we required that these results join smoothly with ENDF data below 20 MeV. We have verified our results in this energy region through comparisons with experimental data and find that they are comparable or superior to existing ENDF evaluations. Finally, in addition to the nuclei listed in Table 1, we are currently producing a library for n+^{238}U reactions up to 100 MeV. Calculations of most cross sections have been completed using new Los Alamos (n,f) data [11] extending to 400-500 MeV and efforts are now under way to calculate fission neutron and gamma-ray production using a preliminary version of a new medium energy fission model developed by Madland.[12] As an example of our data production efforts, Fig. 5 illustrates calculated angle-integrated spectra for neutron, gamma-ray, and charged-particle spectra occurring in n + ^{28}Si reactions.

Table 1. Higher Energy Data Libraries for Transport Calculations

Energy Range	Materials
10^{-11} - 50 MeV*	^{27}Al, ^{54,56}Fe, ^{58,60,62}Ni ^{63,65}Cu, ^{182,183,184,186}W, ^{NAT}Fe, ^{NAT}Ni
10^{-11} - 100 MeV	^{1}H, ^{12}C, ^{16}O, ^{27}Al, ^{28}Si, ^{40}Ca, ^{56}Fe

*Also completed for incident protons

Utilizing New Libraries in MCNP

In applying these new theoretical models to high-energy neutron transport calculations, it is important to include the effects of correlations between the energy and emission angle of secondary neutrons. Typically, the high-energy neutrons have forward-peaked angular distributions, while the low-energy neutrons are emitted in a more isotropic manner. The work of Kalbach and Mann[13] and Kalbach[7] have shown that this energy-angle correlation can be described well for the energies of interest using simple analytic functions of incident energy E, secondary energy E', precompound fraction r(E,E') (which varies from 0 to 1), and the neutron separation energy from the liquid drop model B_b. In designing the new ENDF-B-VI version of the format for the Evaluated Nuclear Data Files, we included an option for recording the factor r(E,E'), along with the differential cross section σ(E,E'). GNASH can be used to produce evaluations using this option, and these evaluations are the basis for subsequent applications.

In order to use these evaluations for neutron transport calculation with the Los Alamos continuous-energy Monte Carlo code MCNP,[14] it was necessary to devise a new scheme for sampling from the energy-angle distributions in the new ENDF files. Such a scheme follows from the Kalbach angular distribution when it is written in the form

$$f(\mu) = \frac{a}{2\sinh(a)}\left[(1 - r)\cosh(a\mu) + re^{a\mu}\right] .$$

MCNP first samples a value for E' using the existing methods designed for simple energy distributions. This E', together with the incident energy E, determines the values of r and the angular distribution slope, a. Next, select a random number R_1. If $R_1 > r$, use the "cosh" part of the distribution in the following way: select a second random number R_2, and then emit the neutron with cosine

$$\mu = \frac{1}{a}\sinh^{-1}\left[(2R_2 - 1)\sinh a\right] .$$

Otherwise, if $R_1 \le r$, use the exponential part of the distribution by selecting a random number R_2 and emitting the neutron with cosine

$$\mu = \frac{1}{a}\ln\left\{\left[R_2e^a + (1 - R_2)e^{-a}\right]\right\} .$$

The parameter a is precomputed in the ACER module of the NJOY nuclear data processing system[15] while it is preparing the other MCNP cross sections in ACE format (A Compact ENDF). The r and a parameters are added to the ACE library using a new format "law."

When the cross section library is read by MCNP, these parameters make it easy to produce neutrons randomly that have the desired energy-angle correlation.

This scheme has the following advantages: it is simple and fast, the data tables are compact, and the calculation takes advantage of existing routines for sampling from energy distributions.

Two other modifications have been made to MCNP in connection with ENDF/B-VI representations of higher-energy data. First, neutron reactions other than fission may now produce a number of secondary neutrons dependent on the incident neutron energy. Second, discrete and continuum secondary photons may now be combined in one distribution.

All MCNP changes described above are required as preliminary steps in the project to generalize MCNP from a neutron/photon code to a true n-particle code.[16] The ultimate goal of that project is to allow transport calculations of arbitrary, user-selected combinations of coupled particles.

Benchmark Calculations

Two simple problems have been used for benchmark calculations of the new libraries. Three sets of calculated results are provided: (1) MCNP Monte Carlo calculations using the data described in this report, (2) results from HETC,[17] an intranuclear cascade Monte Carlo code, and (3) ONEDANT[18] discrete ordinates calculations using the HILO[19] library.

The first benchmark is a test of 100-MeV source neutrons transported through an aluminum sphere. The source is isotropic in the center of a 30-cm radius void. Aluminum (density = 2.699 g/cm^3) fills the remainder of a 75-cm radius sphere. Calculated neutron flux averaged over the outer sphere is shown in Fig. 6. Similarly, the calculated neutron-induced gamma flux is shown in Fig. 7. For the neutrons, the HETC and ONEDANT results are in good agreement. The MCNP results using the new 100-MeV libraries are substantially lower from 15-90 MeV. The MCNP gamma results tend to lie between the ONEDANT and HETC values.

The second benchmark again employs a 100-MeV neutron source. The geometry is identical to that described above, with the exception that the aluminum has been replaced by concrete. This provides a more realistic test of the new data. MCNP and ONEDANT results for the neutron flux averaged over the outer sphere are shown in Fig. 8. The spectral shape is in reasonable agreement; the magnitude of the MCNP results is generally lower, especially from 15-90 MeV.

Summary

Extensive theoretical model development has occurred. The models have been incorporated into the GNASH nuclear model code system. Verification of GNASH predictions by comparing with experimental results for incident neutrons and protons has been accomplished. Complete evaluations in the ENDF/B-VI format have been produced for a number of materials using the new theoretical models, and extending the upper energy limit to 100 MeV. The NJOY processing system has been modified to correctly handle the ENDF/B-VI format used to tabulate the GNASH results, particularly the energy-angle correlations so important in the 20-100 MeV range. The MCNP Monte Carlo code has been modified to accept the new data and sample from new types of distributions. Simple benchmark calculations have been presented, comparing results using the new data library with results based on the intranuclear cascade model. Significant differences are indicated in the 20-100 MeV energy range.

The upper energy limit of 20 MeV traditionally found in ENDF evaluations has proved to be a limiting factor in applications such as accelerator shielding and radiotherapy. Format modifications included in ENDF/B Version 6 have been designed to remove the 20-MeV limitation. The work described in this paper is an attempt to take advantage of the new format in a way that will ultimately be useful to the general community of transport code practitioners.

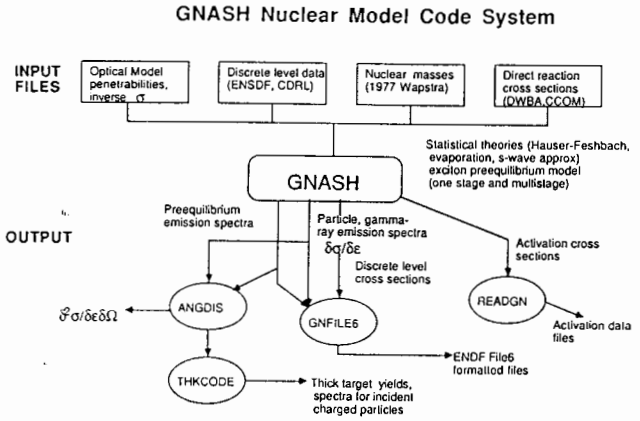

Fig. 1. An illustration of the GNASH nuclear model code system used to produce the results discussed in this paper.

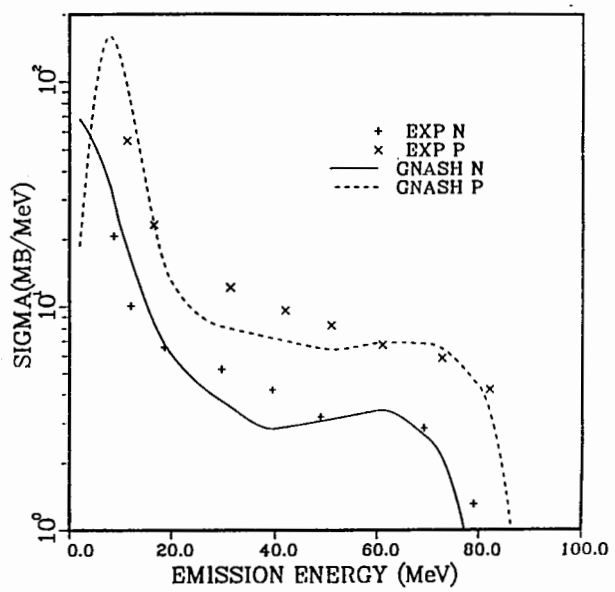

Fig. 2. Angle-integrated proton and neutron production spectra for 90-MeV proton reactions on ^{58}Ni using the methods described in the text are compared with the data of Kalend.[6]

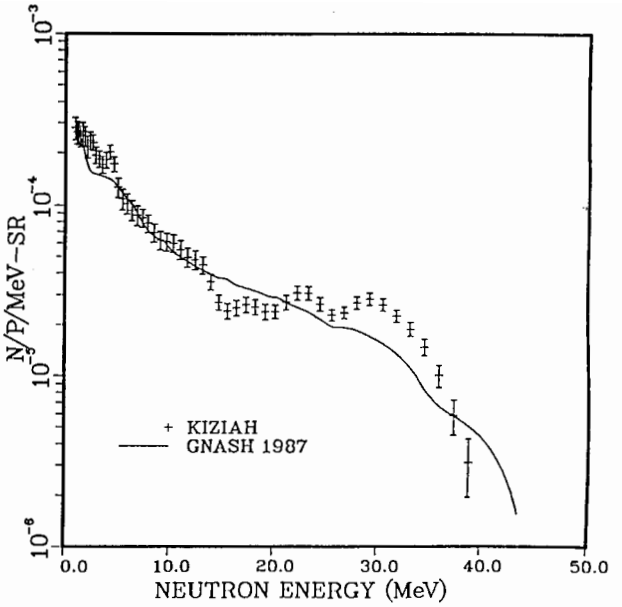

Fig. 3. The thick-target neutron spectral yield at 30° resulting from the stopping of 50-MeV protons in an aluminum target is compared with the data of Kiziah.[8]

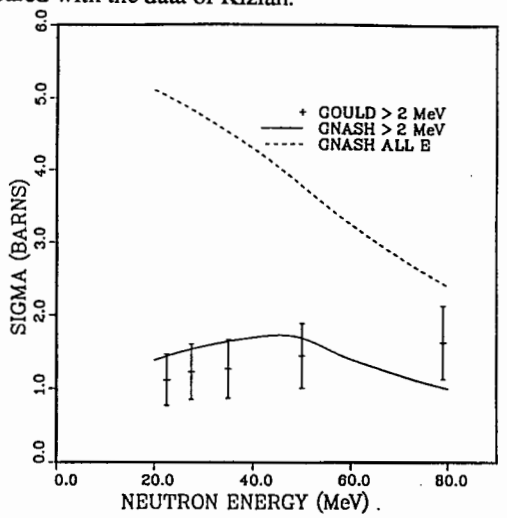

Fig. 4. The calculated gamma-ray production cross section for Ta(n,xγ) reactions with E_γ >2 MeV are compared with results from Ref. 10 in the neutron energy range from 20 to 100 MeV. Also shown by the dashed curve is the total gamma-ray production cross section obtained from the present calculations.

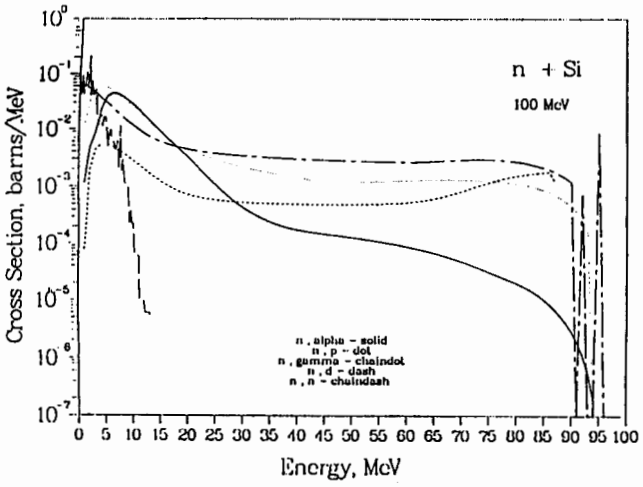

Fig. 5. An illustration of angle-integrated neutron charged-particle, and gamma-production spectra for 100 MeV n+^{28}Si resulting from the present calculations.

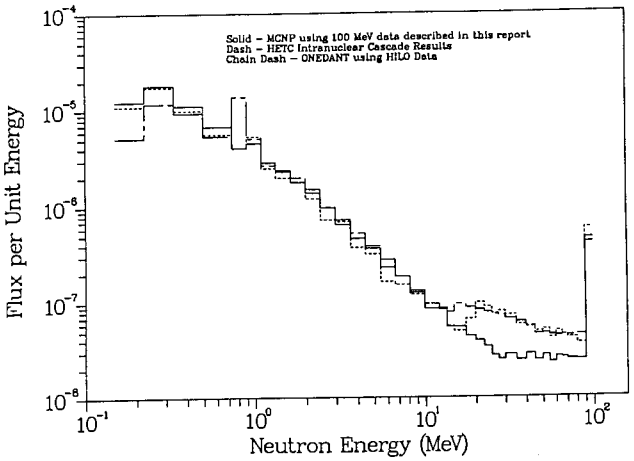

Fig. 6. Comparison of three calculations of neutron leakage fluxes from a 100-MeV neutron source through a 45-cm thick aluminum shell.

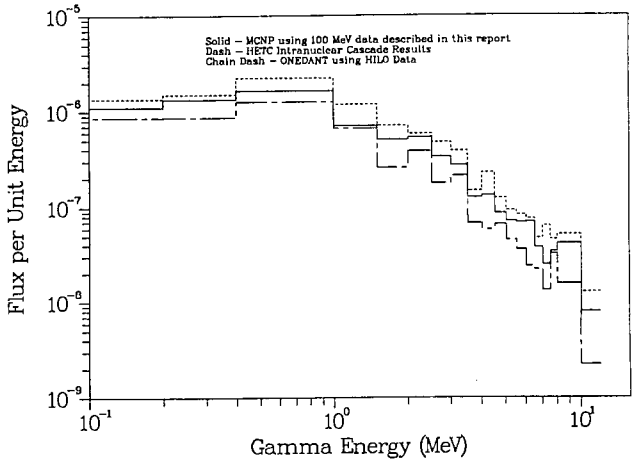

Fig. 7. Comparison of three calculations of neutron-induced gamma fluxes from a 100-MeV neutron source through a 45-cm thick aluminum shell.

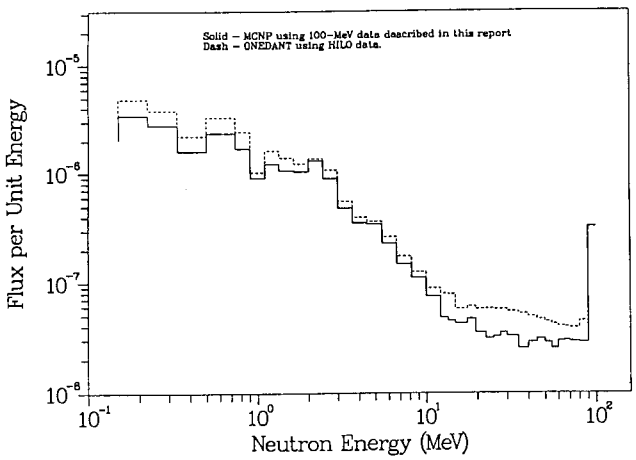

Fig. 8. Fluxes from concrete sphere calculations - MCNP, using T-2 cross sections, and ONEDANT, using HILO cross sections.

References

1. P. G. Young and E. D. Arthur, Los Alamos Nat. Lab. report LA-6947-MS (1977) and E. D. Arthur, Los Alamos informal document LA-UR-88-382 (1988).
2. E. D. Arthur et al., "New Developments in the GNASH Nuclear Theory Code," contribution to this conference A156-R268-B (1988).
3. D. G. Madland, Los Alamos Nat. Lab. informal document LA-UR 88-376 (1988)
4. M. Blann and M. Beckerman, Nucleonika 23, 1 (1978).
5. R. E. MacFarlane in Los Alamos Nat. Lab. report LA-10513-PR (1985).
6. A. M. Kalend et al., Phys. Rev. C 28, 105 (1983).
7. C. Kalbach, Los Alamos informal document LA-UR-87-4139 (1987)
8. R. Kiziah et al, Air Force Weapons Lab. report AFWL-TR-87-63 (1988).
9. S. A. Wender et al., Los Alamos informal document LA-UR-87-3058 (1987).
10. R. Ramakrishnan et al., Nucl. Sci. Eng. 98, 348 (1988).
11. P. W. Lisowski et al., Bull. Am. Phys.Soc. 33, 1063 (1988).
12. D. G. Madland, Applied Nucl. Sci. Group, Los Alamos Nat. Lab. internal report T-2-IR-88-1 (1988) (restricted distribution).
13. C. Kalbach and F. Mann, Phys. Rev. C 23, 112 (1981).
14. J. F. Briesmeister, Ed., Los Alamos Nat. Lab. report LA-7396-M, Rev. 2 (Sept. 1986).
15. R. E. MacFarlane, D. W. Muir, and R. M. Boicourt, Los Alamos Nat. Lab. report LA-9303-M (May 1982).
16. D. J. Brenner, R. E. Prael, and R. C. Little, "Neutron Secondary-Particle Production Cross Sections and Their Incorportation into Monte Carlo Transport Codes," 6th Symp. Neutron Dosimetry, Nueherberg, FRG, Oct. 1987.
17. R. E. Prael and H. Lichtenstein, "User Guide to the HETC Code System," Los Alamos Nat. Lab. Group X-6 Interim Documentation (Oct. 30, 1986).
18. R. D. O'Dell, F. W. Brinkley, Jr., and D. W. Muir, Los Alamos Nat. Lab. report LA-9184-M (Feb. 1982).
19. R. G. Alsmiller, Jr., and J. Barish, Nucl. Sci. Eng. 69, 378 (1979).